Current limiting algorithms and transient stability analysis of grid-forming VSCs

Taoufik Qoria, François Gruson, Fréderic Colas, Xavier Kestelyn, Xavier Guillaud

Version of Record: https://www.sciencedirect.com/science/article/pii/S0378779620305290
Manuscript_a96e24339022fb5644c686f3989ddb15

Study of the tensile behaviour of tungsten wires from ambient temperature to 320°C in relation to their microstructure

R. Michel, Y. Bienvenu, A. Chesnaud and A. Thorel

MINES ParisTech, PSL Research University, Centre des Matériaux (CMAT),
CNRS UMR 7633, BP 87, 91003 Evry, France

Abstract

The tensile test results have been interpreted in terms of the microstructure typical of drawn tungsten wires; the influence of test temperature between 25°C and 320°C is significant and is linked to the dependence of the mechanical behaviour of tungsten versus temperature and to the development with increasing temperature of a necking zone in which damage and rupture take place in two stages, a localized damage controlled first by the hoop stress associated to the notch effect linked to necking and rupture under the axial stress and the notch effect just mentioned.

* Corresponding author: alain.thorel@mines-paristech.fr
Keywords: Tungsten wire, microstructure, texture, tensile fracture mode,

1. Introduction

For more than a century, tungsten wires have played a major role in many industrial applications. They have been used in incandescent lamps for the first time in 1903 [1], in the form of thin wires, replacing carbon filaments obtained earlier from carbonization of cotton or bamboo fibres in the light bulbs produced since 1880. With the highest melting point of all metals (3422°C), a high density of about 19.3 g/cm^3 at 20°C [2], along with an outstanding dimensional stability, tungsten (W) is an essential element for applications that require a high operating temperature. It is the most refractory material in the body centered cubic (BCC) family of metals. This hard metal is brittle and difficult to work. Moreover, after working at ambient temperature (drawing in the case of metal wires), the material is enriched in defects, cracks, and notches, then enhancing its brittleness and inhibiting its workability. In order to solve this problem, one solution is to raise its ductility by introducing alloying elements such as rhenium or potassium [3–7]. But in that case, alloying additives have a deleterious effect on the electrical, chemical and physical properties, which may be unacceptable for many applications. The second solution is to increase the brittle-to-ductile transition temperature domain (DBTT) and work wires under high temperatures; nevertheless, oxidation of tungsten takes place above 400°C, making the shaping difficult without a controlled inert atmosphere [8–10]. Therefore, this paper aims at determining reasonable shaping conditions of stress and temperature to avoid both tungsten wire oxidation and brittleness.

2. Materials and Methods

2.1. Tungsten wires

A circular section tungsten wire from Osram-Sylvania, 400 µm in diameter with a nominal purity level of 99.9% was provided by an industrial partner. The heat treatment history of the wire is not reported precisely but is mentioned as being associated with a limited recrystallization at a temperature close to 1000°C .

2.2. Observation / SEM Analysis

The microstructure of the wires was observed by scanning electron microscopy before and after tensile tests conducted up to rupture using a Zeiss Sigma 450 SEM. The micrographs were collected at an operating voltage of 10 kV and a working distance of 4.9 mm. Samples, observed perpendicularly to the cross-section, were mounted in resin, polished (silicon carbide papers and diamond paste down to a 1 µm grade) and chemically etched in Murakami reagent (1 g KOH + 1 g ($Fe(CN)_6K_3$)). Samples were gold-palladium coated prior to SEM observations.

2.3. Electron BackScatter Diffraction (EBSD)

EBSD images were recorded using an EDAX OIM Hikari rapid acquisition system of crystallographic orientation mapping. The fast camera is equipped with a CCD 640×480 voxels resolution allowing a maximum acquisition/indexing speed of 320 pictures per second (binning: 10×10). The data acquisition and processing were carried out with the IOM Suite v6.1 software. The sections of the tungsten round wires drawn were identified according to their normal axis: sections perpendicular to the axial direction and sections parallel to the axial direction. Both parallel and perpendicular sections were studied in EBSD. To complete the analysis of the as delivered wires, a recrystallized wire was also investigated after annealing at 1600°C for 1 hour under wet H_2/Ar.

2.4. Observation / TEM analysis

TEM observations were performed using a FEI equipment (Tecnai F20-ST) operating at 200 kV and equipped with various detectors as X-microanalysis and HAADF imagery. The conventional images were collected by a high-angle charge-coupled device (CCD) camera with a resolution of 11 Mpixels.

2.5. Tensile tests on W wires

Tensile tests allow determining the elastic and plastic behaviours of a material better than compressive tests and this is especially true for wires, with an aspect ratio length/diameter such that they exhibit poor buckling resistance and poor ability (possibly no ability at all technically) for compressive tests. Tensile tests also allow to establish the material

macroscopic behaviour (until maximum stress is reached) and to obtain the breaking resistance. Uniaxial tensile tests were conducted to acquire stress-strain curves by using a universal testing machine with an optical extensometer and a gauge length of about 100 mm. A sketch of the testing configuration is shown in Figure 1. The tensile tests were carried out at various temperatures (25, 100, 200 and 320°C). The upper testing temperature was limited to 320°C in order to avoid tungsten oxidation, especially the formation of volatile tungsten suboxides like WO_3.

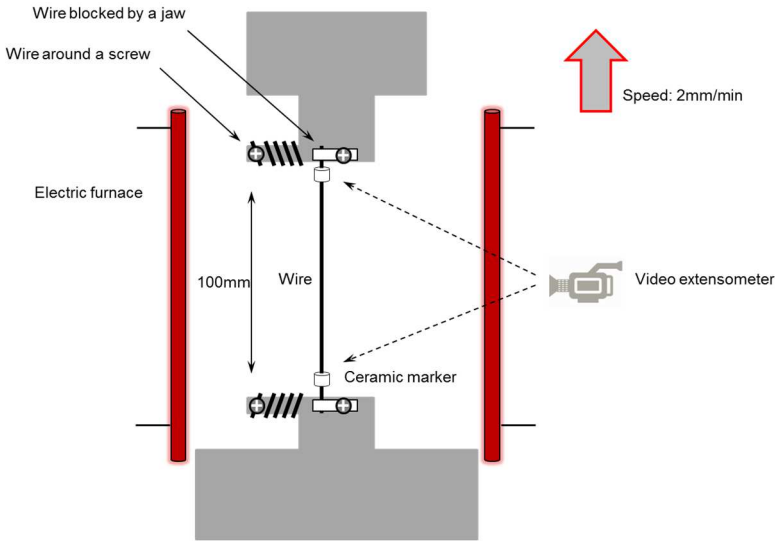

Figure 1: A schematic of the tensile testing configuration.

3. Results and discussion

This section is divided into two parts: the first one covers the microstructural characterization of the tungsten round wires and the results from the electron microscopy analysis including EBSD are evaluated in different manners to achieve a thorough analysis of the microstructure while the second presents the mechanical test results on wires.

3.1. Characterization of tungsten round wire: microstructure and texture

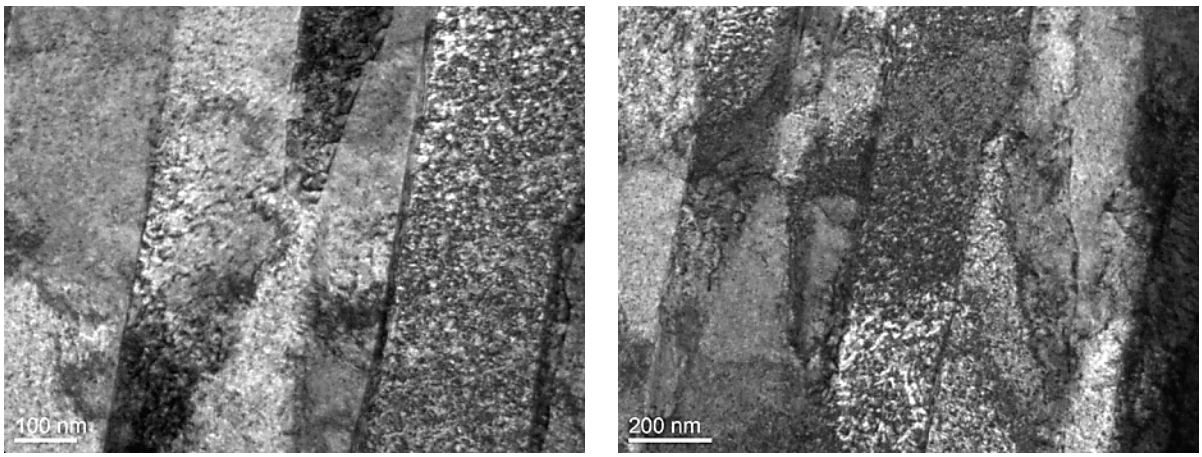

Figure 2: Microstructure of drawn tungsten recorded by TEM using the bright field mode (the sample plane is parallel to the longitudinal axis).

The microstructure of tungsten presents stretched and elongated grains (Figure 2), characteristic of drawn material observed on slices parallel to the longitudinal axis (drawing direction).

Figures 3 and 4 present SEM image and EBSD mapping of the structure of tungsten wire sections perpendicular to the longitudinal axis. Figure 5 and Figure 6 present the SEM image and EBSD mapping of the structure of tungsten wire parallel to the longitudinal axis. The wire axis is predominantly aligned with one <110> plane of the bcc structure and the "fibre" size is of the order of 1 µm. This is confirm to the representation of the structure of as drawn tungsten wire given by P. Schade in his review "100 years of doped tungsten wire" [3]. Cleavage is often hard to distinguish on rupture surfaces of wires due to the roughness of the wire surface and is better evidenced on the rupture surfaces of tungsten sheets as is the case in the work by Wronski and Fourdeux [11].

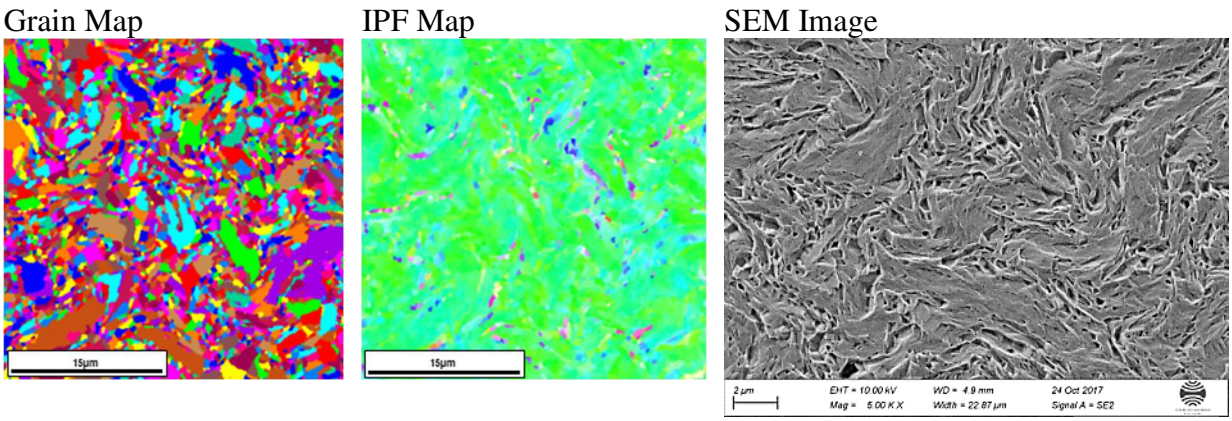

Figure 3: EBSD characterization of the tungsten round wire structure before annealing: sections perpendicular to the wire axis.

The IPF (Inverse Pole Figure) presented as [001] maps in view along the rolling direction.

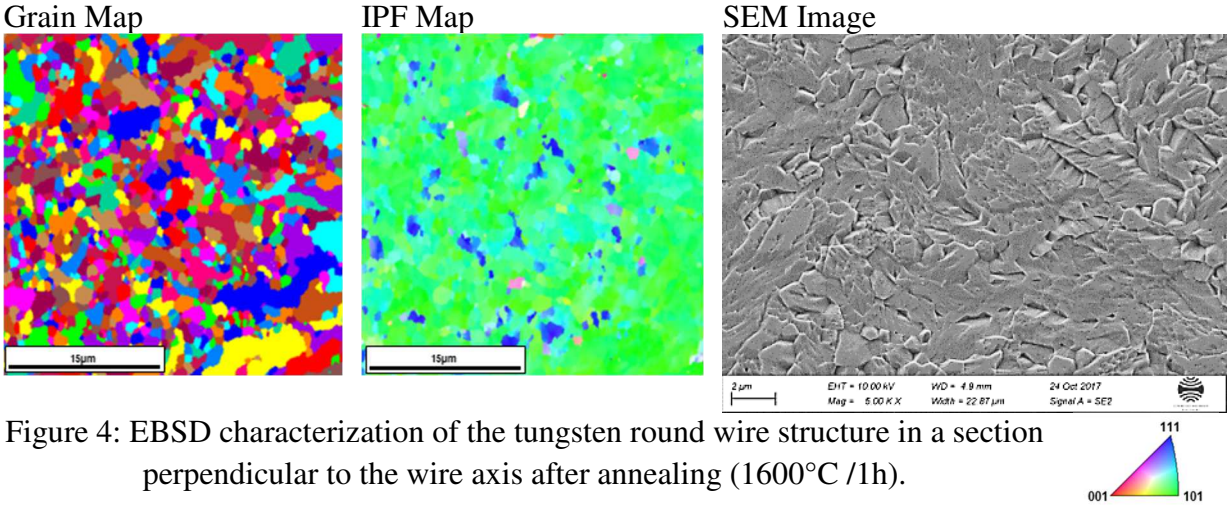

Figure 4: EBSD characterization of the tungsten round wire structure in a section perpendicular to the wire axis after annealing (1600°C /1h).

The IPF (Inverse Pole Figure) presented as [001] maps in view along the rolling direction.

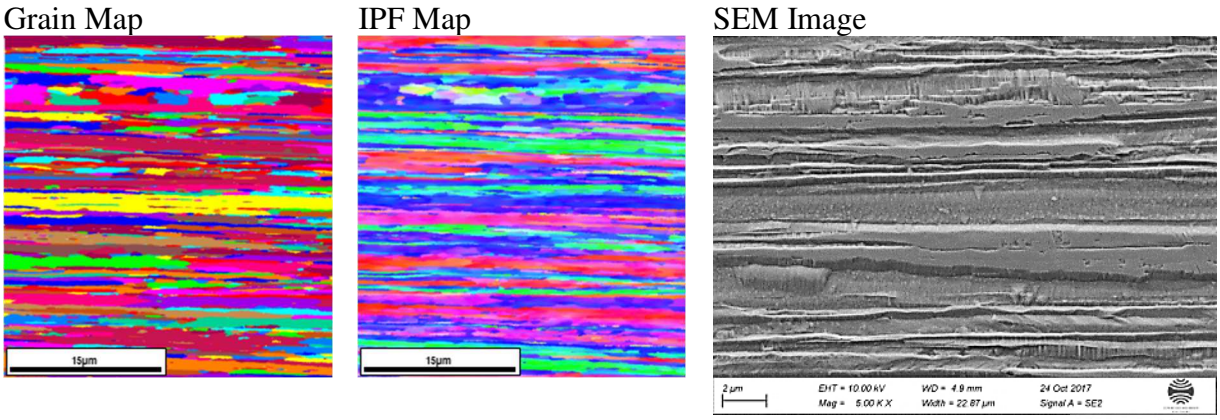

Figure 5: EBSD characterization of the tungsten round wire structure before annealing in a section parallel to the wire axis.

The IPF (Inverse Pole Figure) presented as [001] maps in view perpendicular to the rolling direction.

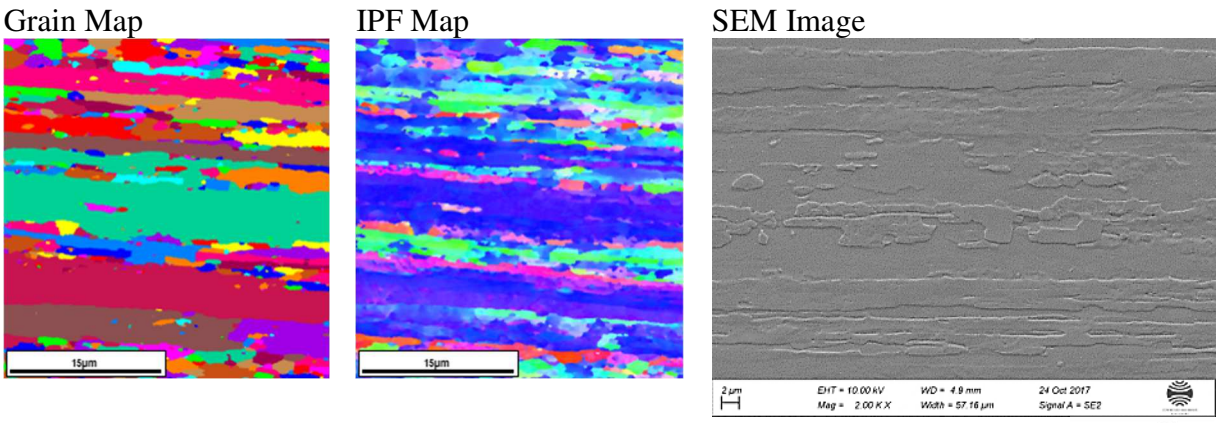

Figure 6: EBSD characterization of the tungsten round wire structure after annealing in section parallel to the wire axis (1600°C /1h).

The IPF (Inverse Pole Figure) presented as [001] maps in view perpendicular to the rolling direction.

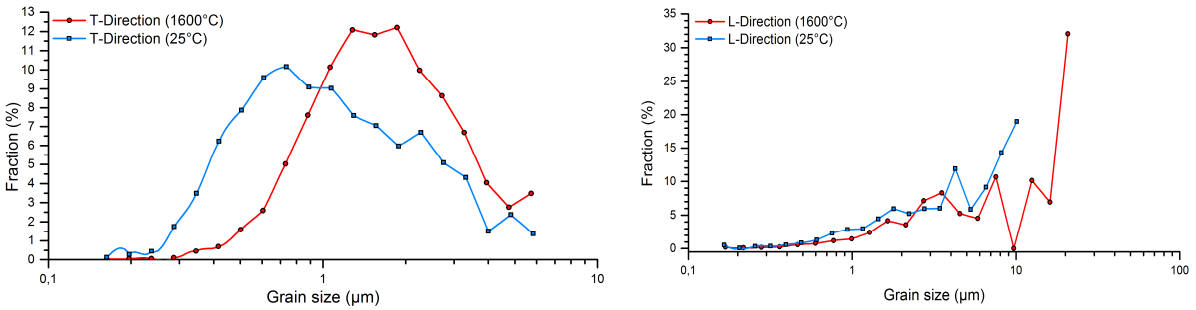

Figure 7: Grain sizes distribution of the drawn round tungsten wires prior and after annealing at 1600°C.

Drawn wire exhibits winding grains with different shapes and a high degree of deformation in L-sections. After annealing, the grains are larger perpendicularly to the deformation axis and more regular; the recrystallization annealing has modified the length/with aspect ratio of grains. Concerning the T-sections, annealing leads to grain coarsening. These results are confirmed in Figure 7. The IFP reveals a good textural development. There is little difference to the privileged crystallographic directions. Along the axial direction, the crystallographic direction [101] is dominant (Figure 8), while in a direction perpendicular to the axial direction these are the [001] and [111] which are the most frequent (Figure 9), the latter direction being more pronounced after annealing.

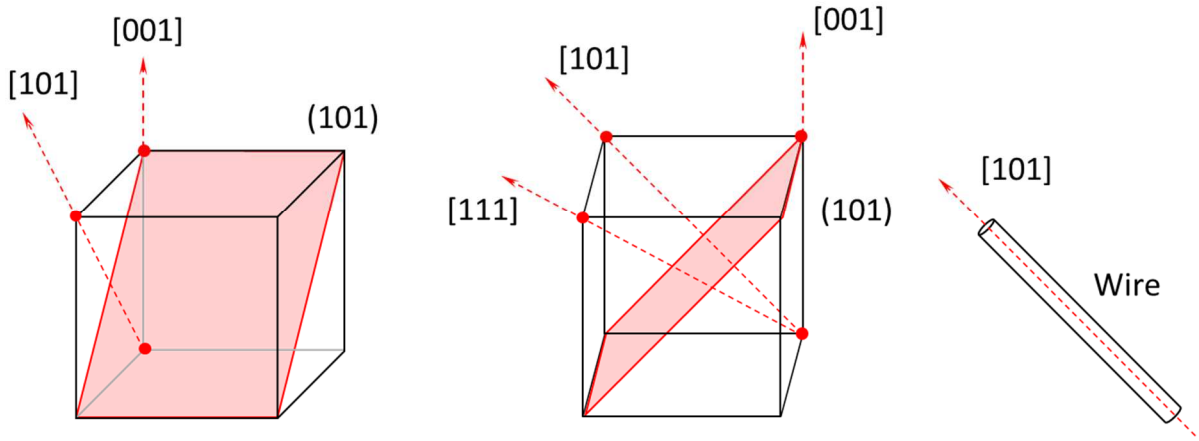

Figure 8: Crystallographic direction along the drawing direction.

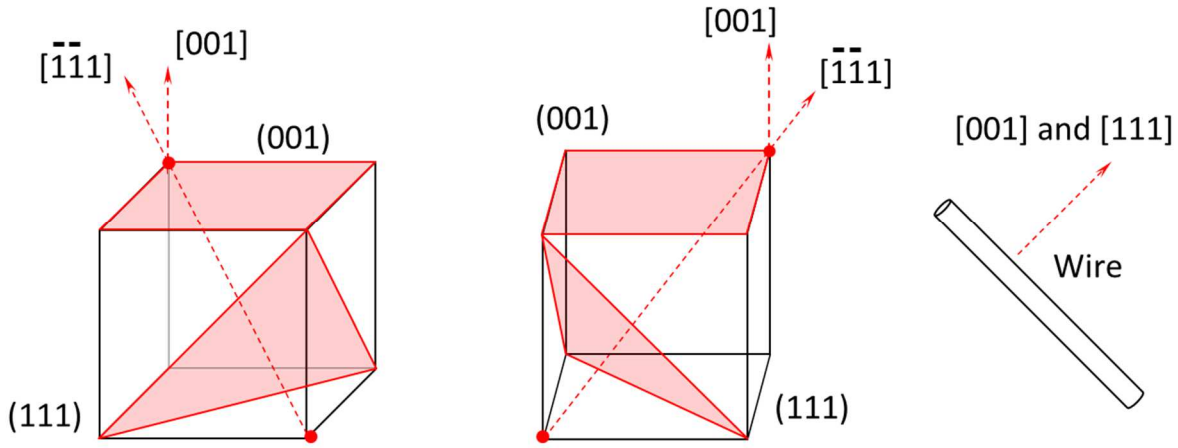

Figure 9: Crystallographic direction in a perpendicular direction to the drawing direction.

3.2. Tensile tests results and fracture modes

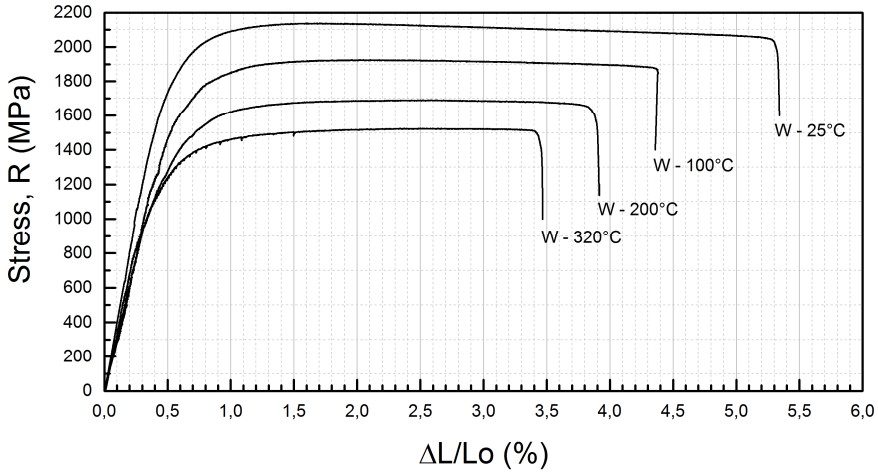

Figure 10: Stress-strain curves of round tungsten wire 400 µm in diameter at temperatures ranging from ambient to 320°C.

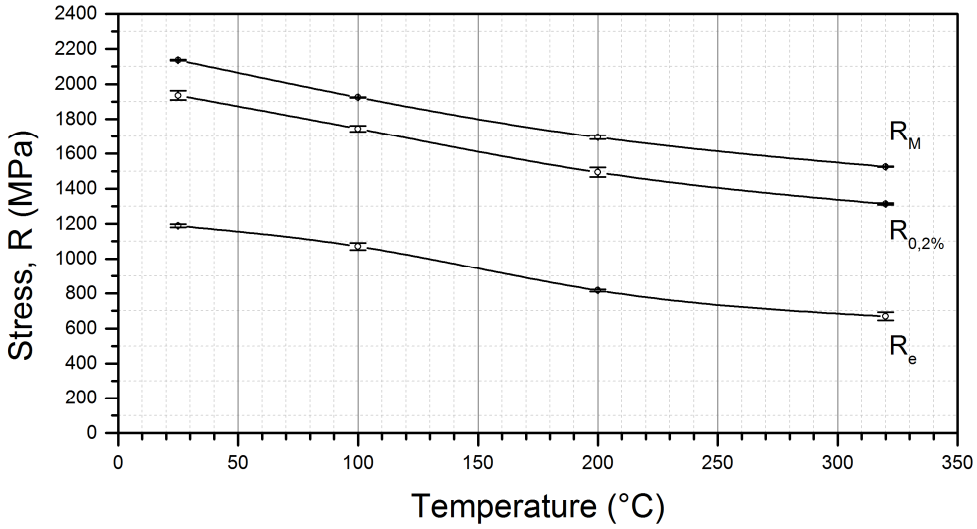

Figure 11: Tensile strength R_M, "true" yield stress R_e and conventional elastic limit $R_{0.2\%}$ as a function of testing temperature.

Figure 10 illustrates typical stress-strain curves obtained with the as received tungsten wires at different temperatures. Moreover, the tests were repeated 3 times to assess reproducibility. Figure 11 presents the tensile strength R_M, "true" yield stress R_e and conventional 0.2% elastic limit $R_{0.2\%}$ as a function of the temperature. The reductions in area at rupture (RA) measured from micrographs in Figures 12 and 13 are reported in Table 1 together with rupture elongations (A%)

Table 1: Reductions in area at rupture and rupture elongations

Temperature	25°C	100°C	200°C	320°C
Reduction in area (%)	20	43	48	55
Elongation (%)	5	4	3.5	3

According to Zerilli's review of Dislocation Mechanics–Based Constitutive Equations applied mostly to high strain rate mechanical behaviour of metals [12], for bcc metals dislocation-lattice interaction is predominant and the yield stress is temperature dependent while strain hardening is thermal, as suggested by our results in the 25°C/ 320°C temperature range. The Johnson-Cook based constitutive equation relating Von Mises stress and strain was modified by Armstrong and Zerilli to account more closely for the experimental yield stress temperature dependence for bcc metals. One way was to add above a critical stress value a contribution of deformation twinning in addition to the dislocation glide. Wronski and Fourdeux [11] also suggested this combination of deformation mechanisms leading ultimately to a rupture by cleavage at 77K.

A comparison of present tensile test results with those found in the literature for pure tungsten in the form of wires of diameter close to 400 µm and also of extruded rods is of some interest. The majority of the references used date back to the 1960's. The compilation of the properties of tungsten by the Battelle Memorial Institute [13] leads us to propose that our wire effectively belongs to the category of wires of a similar diameter annealed at a temperature lower than 1000°C, resulting in a ductile brittle transition temperature below ambient temperature but the decrease in the elongation at rupture we measured is not in agreement with the stability with increasing temperature of this property, around 5%, reported in this compilation. Sell from Westinghouse Lamp Division in his review of the advanced processing of tungsten alloys and of their high temperature mechanical properties [14] devotes a few pages to the parameters influencing the ductile brittle transition temperature and to the "low" (<1000°C) temperature mechanical properties and concludes that if grain size is small (our case and the usual case of tungsten wires), heat treatment (HT) at temperatures >1000°C affects predominantly the low temperature strength and ductility of unalloyed tungsten through the distribution of impurities at grain boundaries. Terentyev et al. [15] performed tensile tests on pure W wires, 150 µm in diameter over a temperature interval ranging from ambient to 600°C and obtained ultimate strength and reduction in area figures for the as drawn wires similar to ours and reported elongation figures lower than ours but steadily decreasing from 1,6% to 1% with increasing temperature. However the reduction in area figures of Terentyev et al. [15] are quite comparable to ours. Union Carbide, E.I. Harmon et al [16] performed their tensile tests in the temperature range ambient to 1925°C on extruded pure tungsten rods about 4 mm in diameter fabricated by swaging arc melted tungsten and reported ultimate tensile strengths about half of ours between ambient temperature and 320°C but significantly higher elongation values than those reported here. This can be explained by the difference in deformation and work hardening to produce a 400 µm diameter wire and a rod with a 10 times bigger diameter. In the temperature range 250°C/1925°C, Harmon et al reported values of rupture elongation and reduction in area that are respectively decreasing and increasing with test temperature, as we do over a lower temperature range. These

observations suggest that rupture elongation is controlled by work hardening, strain aging and more specifically by their variations with temperature. This induces us to consider work hardening during tensile testing; this is why, in addition to the 0.2% offset yield stress, we attempted to determine a "true" yield stress (Figure 11).

In spite of a limited rupture elongation the strain hardening is large, about as large as the "true elastic" limit. A typical value of the strain hardening for 1% plastic deformation for our wire at room temperature is about 1 GPa while P.L. Raffo reports about 0.13 GPa for high temperature annealed W rods about 4 mm in diameter fabricated from arc melted buttons [5]. The discrepancy between our values of the strain hardening for 1% plastic deformation and those presented by P.L. Raffo is likely to be due to the fact that we use the "true yield stress and not the conventional 0,2% Yield stress like Raffo. Our values for strain hardening do not show a well-defined temperature dependence, while P.L. Raffo reports a decrease of strain hardening with temperature [5].

At room temperature, the wire breaks in a plastic mode of deformation and presents the highest rupture elongation of the series. The rupture elongation decreases with increasing temperature (Figure 11) and a good level of reproducibility can be noted.

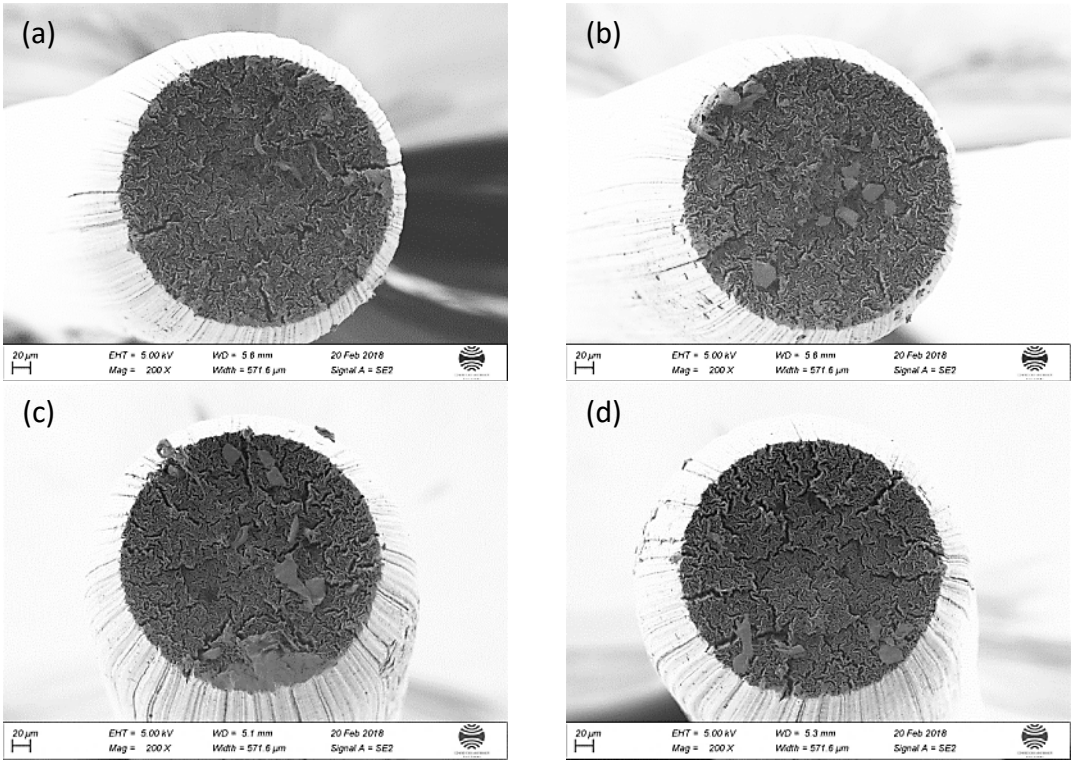

Figure 12: Fracture surface of tungsten wires at two different temperatures, (a) and (b) at 25°C; (c) and (d) at 100°C.

The wires rupture elongation decreases together with rupture stress with increasing temperature (Figure 10) while the cross sectional "necking" reduction in area increases (Table 1). Actually, the wire presents a rather uniform deformation and elongation at RT safe for a small striction zone while a more pronounced local ductile deformation is observed at higher temperatures in the striction (also called necking) zone with obviously a biaxial stress field (axial and hoop stresses) with possibly a triaxial state of stress in W at some distance

beneath the surface of the striction zone. Intergranular delamination under the hoop stress component seems to be initiating damage leading to rupture. The latter is of the intragranular type with the fracture surface roughly perpendicular to the axial direction. The initiation site of cracks on the wire surface is presumably longitudinal grooves separating neighbouring grains. This defect acts as an additional stress concentrator for the hoop stress.
Note that the "radial" delamination openings observed on the rupture surface propagate in the axial direction on both sides of the rupture surfaces but not beyond the root of the striction zone (Figure 12 and 13). Below 200°C (Figure 12), a rather large number of intergranular delaminations is observed on the rupture surface while, at 200°C and 320°C (Figure 13), fewer but more opened and deeper delaminations can be clearly distinguished. Figure 14 and 15 illustrate in more details the intergranular nature of the crack (delamination) propagation paths: well developed more or less radial cracks are observed following the wavy W grain boundaries.

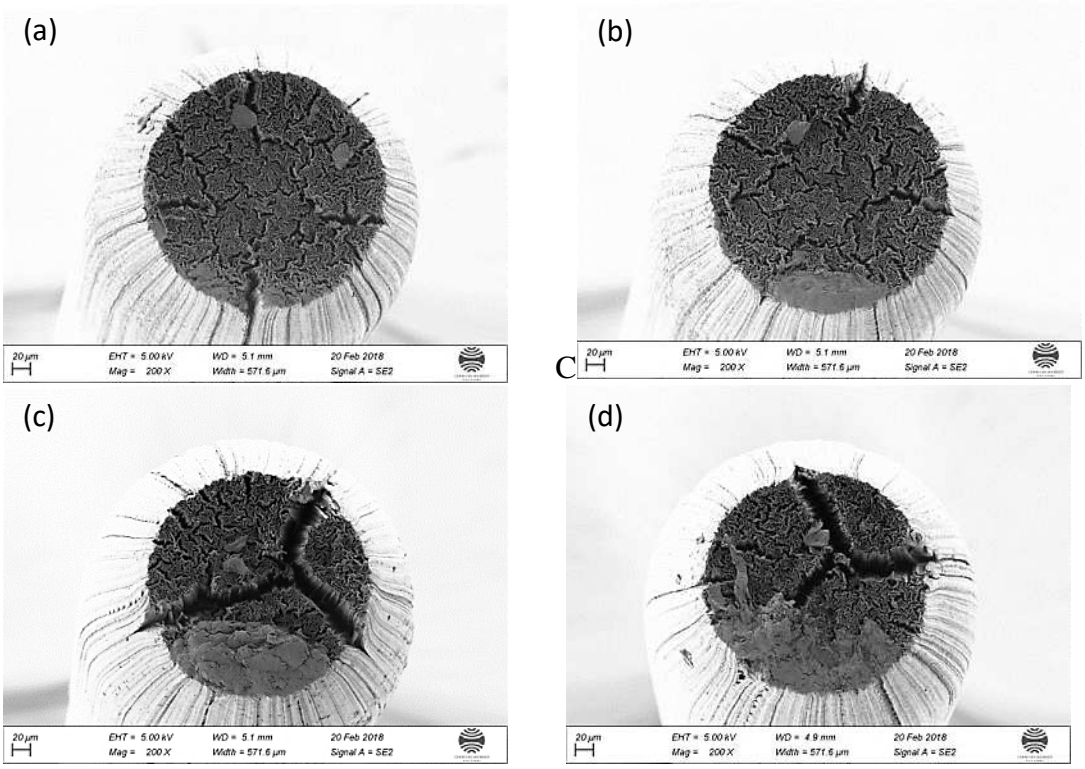

Figure 13: Fracture surface of tungsten wires at different temperatures at (a) and (b) 200 and (c) and (d) 320°C.

At 25°C the final rupture surface reveals longitudinal-radial delamination planes. The cracks are propagating a short distance towards the wire centre and they tend to be wider at the wire surface. Moreover, Figure 14 with fine scale SEM observations confirms that the cracks are due to longitudinal grain delamination along longitudinal W grain boundaries. The microcavities are called knife-edge-necking of grains [17]. At higher temperatures, ductility increases for W in the longitudinal direction and necking of the wire is more pronounced. The size of the longitudinal propagation cracks increases and they also become more opened and wider. Moreover, cleavage appears above 100°C and dominates the edge of the rupture surface as shown earlier by P. Schade [3]. Rather similar observations have been recently

made by D. Terentyev et al [7] who studied the tensile behaviour of a 150 µm diameter W wire recrystallized at 2300°C (presumably much higher than the recrystallization temperature of our as received wires). The tensile strength values they reported are indeed significantly lower than ours although the elongation at rupture figures are about similar and showing similar trends with temperature; nevertheless necking (development of a striction zone) is still more pronounced in the study of D. Terentyev et al [7] above 100°C than what is shown in Figures 12 and 13 of our study.

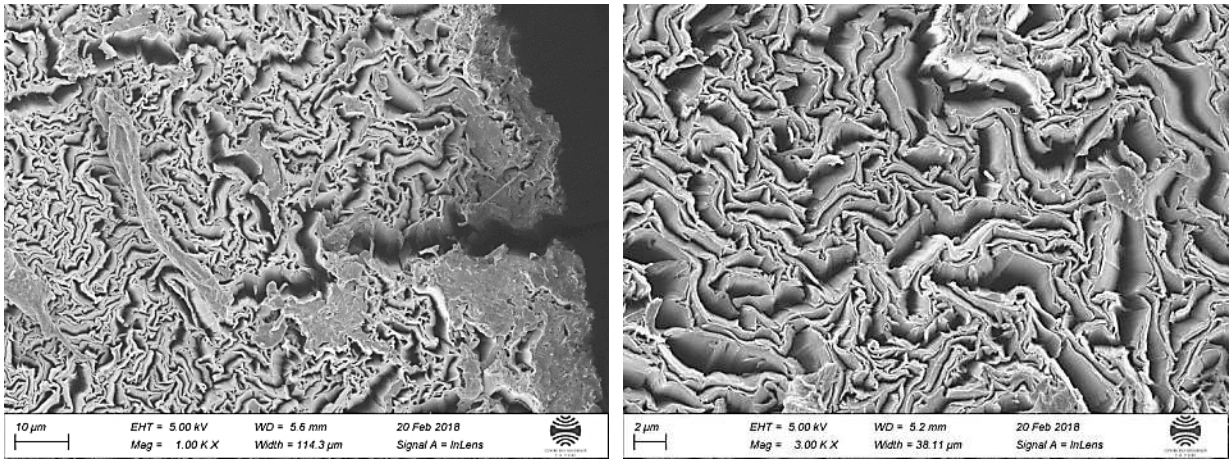

Figure 14: Fracture surface of tungsten wire at 25°C.

The notch effect associated with striction under the axial, loop and radial stresses in the plane at mid-height of the striction zone which is to become the rupture surface can be calculated elastically. Figure 15 represents on the left vertical ordinate axis values of the three stress components relative to average tensile stress, suggesting high values (75% of the average axial stress) for the tensile loop stress associated with a high notch factor for a notch radius equal to 10% of the round bar diameter [18]. Using Figures 12 and 13, we can estimate that in our tensile tests the smallest striction zone "equivalent notch" radius is about 80 µm, i.e. 20% of the wire radius at room temperature and significantly more at higher test temperatures (which means a less pronounced notch effect). Beneath the wire surface a radial tensile stress develops also contributing to the opening of the intergranular cracks. Intergranular decohesion under the effect of the hoop and radial stress can be the first stage in damage followed by the final rupture perpendicular to the tensile axis of the reduced cross section of the wire which can be qualified as a transgranular rupture with some signs of microductility. On the rupture surface several blocks can be seen separated by the intergranular delamination mechanism. Cleavage can also be identified in the peripheral part of the rupture surface.

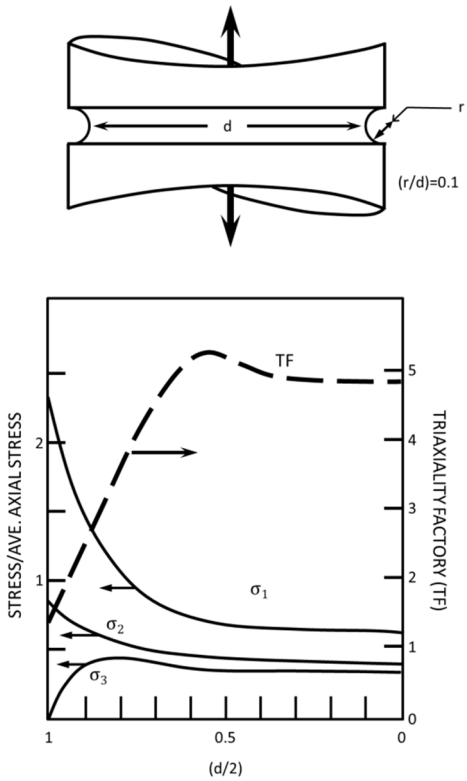

Figure 15: Example of triaxial stress state across a notched round bar obtained from elastic calculations (from D.V. Nelson GE-ARSD quoted by A. M. Agogino [18])

A finite element analysis to calculate striction zone shape and associated stress and strains fields has been proposed by D. Yao et al [19]; for different metals (some of them being not so ductile, like our wires) with different tensile curves but not for tungsten. Calculated striction zones are compared with experimental results [19]. One way for a material to limit striction in a tensile test is to be characterized by a high strain hardening capability. This is the case for our wire which are stronger than the wires of D. Terentyev et al [7] and the W material of P.L. Raffo et al [5] (arc melted and high temperature annealed buttons with large grains). Moreover, the strain hardening of our wires is not significantly reduced with increasing temperature which limits the decreasing trend or the maximum stress with temperature even if the necking effect is more pronounced at higher temperature.

4. Conclusions

The mechanical behaviour of W wires, 400 µm in diameter, has been established from ambient temperature to 320°C through tensile tests. In spite of a limited value of the rupture elongation, typical for W, the strain hardening in just a few % of plastic deformation is quite large. The damage and rupture mechanisms are closely linked to the microstructure of the drawn wire with grains elongated along the drawing/tensile axis. With increasing test temperature, yield stress, maximum stress and rupture elongation decrease while the striction zone becomes more important giving evidence of increasing local ductility. The initial W wire damage mechanism is by intergranular decohesion in the striction zone, presumably triggered

by the relatively high hoop stress associated with the “notch effect” linked with striction zone geometry. The wire surface roughness is also offering many longitudinal grooves facilitation crack openings. Final rupture is about normal to the tensile axis but the previously mentioned intergranular decohesion may explain why the rupture surface is not more planar. The damage mechanisms discussed in the interpretation of the tensile test results also operate in the shaping and working of round W wire by forging, rolling, …, all processes that bring in tension the wire surface not in contact with the tooling.

Acknowledgment

This project has received funding from the European Union’s Horizon 2020 research and innovation programme under grant agreement No° 687316

References

[1] P. Schade, H.M. Ortner, I. Smid, Refractory metals revolutionizing the lighting technology: A historical review, Int. J. Refract. Met. Hard Mater. 50 (2015) 23–30.
[2] D.R. Lide, CRC Handbook of Chemistry and Physics, 84th ed., 2004.
[3] P. Schade, 100 years of doped tungsten wire, Int. J. Refract. Met. Hard Mater. 28 (2010) 648–660.
[4] S. Wurster, B. Gludovatz, R. Pippan, High temperature fracture experiments on tungsten–rhenium alloys, Int. J. Reractory Met. Hard Mater. 28 (2010) 692–697.
[5] P.L. Raffo, Yielding and fracture in tungsten and tungsten-rhenium alloys, J. Less-Common Met. 17 (1969) 133–149.
[6] C.L. Briant, Potassium bubbles in tungsten wire, Metall. Trans. A. 24A (1993) 1073–1084.
[7] D. Terentyev, J. Riesch, S. Lebediev, T. Khvan, A. Zinovev, M. Rasiński, A. Dubinko, J.W. Coenen, Plastic deformation of recrystallized tungsten-potassium wires: Constitutive deformation law in the temperature range 22–600 °C, Int. J. Refract. Met. Hard Mater. 73 (2018) 38–45.
[8] J. Reiser, L. Garrison, H. Greuner, J. Hoffmann, T. Weingärtner, U. Jäntsch, M. Klimenkov, P. Franke, S. Bonk, C. Bonnekoh, S. Sickinger, S. Baumgärtner, D. Bolich, M. Hoffmann, R. Ziegler, J. Konrad, J. Hohe, A. Hoffmann, T. Mrotzek, M. Seiss, M. Rieth, A. Möslang, Ductilisation of tungsten (W): Tungsten laminated composites, Int. J. Refract. Met. Hard Mater. 69 (2017) 66–109.
[9] J. Reiser, S. Wurster, J. Hoffmann, S. Bonk, C. Bonnekoh, D. Kiener, R. Pippan, A. Hoffmann, M. Rieth, Ductilisation of tungsten (W) through cold-rolling: R-curve behaviour, Int. J. Refract. Met. Hard Mater. 58 (2016) 22–33.
[10] A.A.N. Németh, J. Reiser, D.E.J. Armstrong, M. Rieth, The nature of the brittle-to-ductile transition of ultra fine grained tungsten (W) foil, Int. J. Refract. Met. Hard Mater. 50 (2015) 9–15.
[11] A. Wronski, A. Fourdeux, Slip-induced cleavage in polycrystalline tungsten, J. Less-Common Met. 6 (1964) 413–429.
[12] F.J. Zerilli, Dislocation mechanics-based constitutive equations, Metall. Mater. Trans. A Phys. Metall. Mater. Sci. 35 A (2004) 2547–2555.
[13] F.F. Schmidt, H.R. Ogden, The engineering properties of tungsten and tungsten alloys, Battelle Memorial Institute, 1963.

[14] H.G. Sell, G.H. Keith, R.C. Koo, R.H. Schnitzel, R. Corth, Physical Mettallurgy of tungsten and tungsten alloys, WADD Techn, 1961.
[15] D. Terentyev, J. Riesch, S. Lebediev, A. Bakaeva, J.W. Coenen, Mechanical properties of as-fabricated and 2300°C annealed tungsten wire tested up to 600°C, Int. J. Refract. Met. Hard Mater. 66 (2017) 127–134.
[16] E.I. Harmon, Investigation of the Properties of Tungsten and Its Alloys, WADD Tech. Rep. 60-144. (1960).
[17] P. Zhao, J. Riesch, T. Höschen, J. Almanstötter, M. Balden, J.W. Coenen, R. Himml, W. Pantleon, U. von Toussaint, R. Neu, Microstructure, mechanical behaviour and fracture of pure tungsten wire after different heat treatments, Int. J. Refract. Met. Hard Mater. 68 (2017) 29–40. doi:10.1016/j.ijrmhm.2017.06.001.
[18] A.M. Agogino, Notch effects, Stress State, and Ductility, J. Eng. Mater. Technol. 100 (1978) 348–355.
[19] D. Yao, L. Cai, C. Bao, A new approach on necking constitutive relationships of ductile materials at elevated temperatures, Chinese J. Aeronaut. 29 (2016) 1626–1634.